Impact of Optimally Controlled Continuously Variable Transmission on Fuel Economy of a Series Hybrid Electric Vehicle

Boli Chen, Simos A. Evangelou and Roberto Lot

Abstract— This paper investigates energy efficiency of a series hybrid electric vehicles (HEV) that utilizes a continuously variable transmission (CVT) to connect the electric motor to the wheels. In contrast with a fixed transmission (FT) that employs a fixed final drive ratio, the CVT offers variable transmission ratio that can be freely controlled, so that the motor is driven more efficiently. The performance of the CVT is evaluated within an optimal control framework under an urban drive mission, which is specified in terms of the road geometry and the traveling time for the journey. Apart from the CVT operation, vehicle speed and the energy management are also simultaneously optimized by an indirect optimal control method, based on the Pontryagin's minimum principle (PMP). The simulation results illustrate the benefit of the CVT as compared to a fixed transmission in terms of fuel economy.

I. INTRODUCTION

In recent decades, there has been increasing concern about the vehicle emissions, which are main contributors to global warming and air pollution in large urban areas. Significant research has been devoted to hybrid electric vehicles that have been considered the ideal transition from conventional to full electric vehicles. One of the major benefits of hybrid architectures as compared to conventional vehicle architectures is that they allow energy to be recovered and stored temporarily for future use. There are basically three different hybrid architectures: series, parallel and mixed e.g., series-parallel. This article addresses HEVs of series architecture which also include the extended-range electric vehicles in practice, such as the BMW i3 range extender, the Nissan Note e-power and a variety of products from VIA Motors.

Since the wheels only receive mechanical power from the motor in a series HEV, the final drive ratio plays an important role in the motor efficiency, and in turn in the overall powertrain efficiency. This paper investigates the effectiveness of a continuously variable transmission (CVT) in such a series drivetrain in comparison to a widely used fixed transmission. There is a rich literature on the use of CVT for parallel hybrid vehicles, where the CVT also acts as the power split device between the engine and the motor [1], [2], [3], [4], [5]. However, the investigation of CVT for series HEV powertrains is still limited. Recently, the performance of a linearly controlled CVT system is evaluated in a hybrid electric vehicle of series architecture for given drive cycles [6]. The control algorithm is designed such that the motor is operated along a straight line passing through the origin

B. Chen is with the Dept. of Electrical and Electronic Engineering at Imperial College London, UK (`boli.chen10@imperial.ac.uk`).

S. A. Evangelou is with the Dept. of Electrical and Electronic Engineering at Imperial College London, UK (`s.evangelou@imperial.ac.uk`).

R. Lot is with the Dept. of Engineering and the Environment at the University of Southampton, UK (`Roberto.Lot@soton.ac.uk`).

and the point of peak efficiency in the motor efficiency map with respect to the speed and torque. Such linear control strategy offers a computationally efficient solution, however, it relies on an assumption that the optimal operating points can be defined as a linear relationship between motor speed and torque. Therefore, the solution is only suboptimal and the optimality degrades as the accuracy of the linear approximation drops. The benefit of this CVT system in [6] is characterized by the increase in the motor efficiency instead of overall fuel economy because the CVT control is isolated from the energy management strategies.

In contrast with [6], the present paper deals with an optimal control methodology for combined and global optimization of the CVT gear ratio, the power share and the driving speed in terms of fuel consumption. Therefore, the necessity of knowing a priori the driving cycle that is usually not available in real-world driving is removed. Instead, the drive mission is defined by the path whose geometry is taken from *Google Maps*, and the average speed. Thus, the CVT and energy management controls are coupled via the driving speed, and the inclusion of the entire powertrain allows the characterization of CVT performance in terms of overall fuel economy which is much more relevant than the efficiency of single components such as motor or transmission, which was used in [6]. In this paper, the optimal control problem (OCP) is addressed by an indirect optimal control solver named PINS for its competitive accuracy and robustness as compared to the solvers pertaining to other categories [7], such as dynamic programming and nonlinear programming. The utilized indirect approach is based on the Pontryagin's maximum principle which finds the optimal solution by converting the OCP into a two-point boundary value problem.

The paper is organized as follows. The paper first introduces the vehicle model used in this investigation in Section II, including the implementation of a CVT. In Section III, the optimal control problem is formulated. Simulations of given vehicle mission are conducted and the results are presented and discussed in Section IV, and Section V draws some concluding remarks

II. SERIES HEV MODEL

As shown in Fig. 1, the series hybrid electric vehicle is powered by two energy sources including the internal combustion engine (ICE) and the battery. In the branch of primary source, the fuel chemical power P_f is transformed in to the DC electric power P_r via the engine optimal management system, that includes the ICE, generator and the rectifier. The branch of secondary source of energy (SS) consists of the battery and the DC-DC converter. It allows energy recovery either by the primary source or by
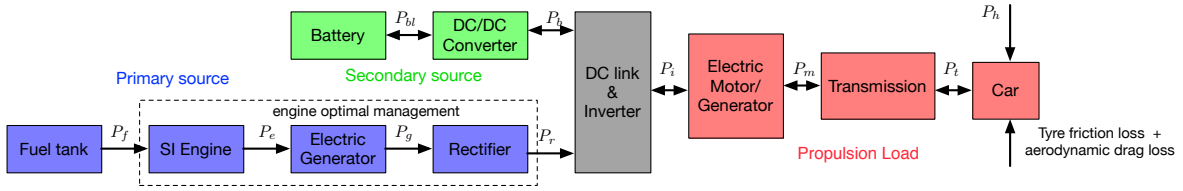
Fig. 1. Block diagram of the series HEV powertrain used in this work.

regenerative braking. The power from both branches (i.e., P_r and P_b) is combined at the DC link and then delivered to the wheel via the inverter, the traction motor and the transmission system. Eventually, the vehicle is driven with P_t, which is positive for propulsion and negative for the regenerative braking. Mechanical brakes are also included to decelerate, with the corresponding power P_h converted into heat dissipation. The energy management consists in optimizing three independent sources of power P_b, P_g, and P_h with the aim of minimizing overall fuel consumption.

The proposed vehicle model represents a medium-size family car of 1500 kg. The mathematical model studied in this paper is described in [8] whereas the fixed transmission is replaced by the CVT. In the following, the vehicle model is briefly reviewed. Noticeably, the power losses due to power conversion precesses are taken into account by transmission efficiencies.

A. Primary source

The vehicle model represents a medium-size family car with a 1.8L petrol engine, that produces a peak power of 86kW at 5000 rpm and a peak torque of 170 Nm at 3950 rpm. The SI engine is directly connected to the permanent magnet synchronous (PMS) generator, which converts the engine power P_e into the electric AC power P_g.

Thanks to the series layout, the engine is not mechanically connected to the wheels. Therefore, different combinations of engine torque and speed may be used to provide the same power. This redundancy gives the possibility of implementing an engine control strategy that maximizes the efficiency of primary source branch. As described in [8], once such strategy has been implemented, the engine fuel mass rate q_f is approximated as linearly dependent on the primary source power output P_r as shown in the following dynamic equation:

$$\frac{d}{dt}Q_f = q_{f0} + \frac{P_r}{Q_{HV}\,\alpha_f\,\eta_r} \tag{1}$$

where Q_f is the depleted fuel mass, and, for the powertrain herein considered, $q_{f0} = 0.23$ g/s is the fuel mass rate to keep the engine idle. Moreover, $Q_{HV} = 44$ MJ/kg is the gasoline heating value, $\alpha_f \simeq 0.32$ is the coefficient of power transformation and $\eta_r = 0.96$ is the efficiency of the rectifier.

B. Secondary source

The Li-ion battery model used in the paper is based on the equivalent electrical circuit presented in [9], [10]. Let i_b denote the battery current, assumed positive during the discharge phase, then the dynamic of the actual battery charge Q_b follows:

$$\frac{d}{dt}Q_b = -i_b \,. \tag{2}$$

The battery state-of-charge (SoC) is defined by

$$SoC = \frac{Q_b}{Q_{\max}} \,, \tag{3}$$

where $Q_{\max} = 5$Ah is the battery capacity. Therefore, the dynamic of SoC is governed by

$$\frac{d}{dt}SoC = -\frac{i_b}{Q_{\max}} \,. \tag{4}$$

The Li-ion battery voltage may be approximated by the following expression:

$$V_b = V_{oc} - R_b i_b \tag{5}$$

where V_b is the closed circuit voltage of the battery, $R_b = 0.2056\Omega$ is the internal resistance and $V_{oc} = 300$V is the open circuit voltage. Therefore, the energy capacity of the battery is 1.5kWh, which is identical to the one used on the series HEV Nissan note e-power. The C-rate limit is set to 8C and 16C respectively for charging and discharging because the small size battery must be capable of delivering continuous currents of 10C or more in practice for sufficient propulsion power. As a consequence, the battery SoC is limited within a small range: 50% – 80% to avoid deep charging/discharging, which would significantly reduce battery cycle life.

The battery voltage is amplified by the DC/DC converter that is simply modelled as a constant efficiency $\eta_{dc} = 0.96$ [11]. Therefore, the bi-directional power conversion via the converter is described by:

$$P_b = \eta_{dc}^{\mathrm{sign}(P_b)} P_{bl} \tag{6}$$

where $P_{bl} = i_b V_b$ is the battery power on the low voltage side, while P_b is the battery power on the DC link side.

C. Transmission branch

1) PMS motor: The power from the primary source P_r is combined with the battery power P_b at the DC link and then converted from DC into AC by the inverter, that is simply modelled as a constant efficiency factor $\eta_i = 0.96$. The power balance of the DC link and inverter is described by the following equation:

$$P_i = \eta_i^{\mathrm{sign}(P_r+P_b)}\left(P_r + P_b\right) \,. \tag{7}$$

The dynamic behaviour of the PMS generator is described in the rotor $d-q$ reference frame [12] by the following nonlinear differential equations:

$$L_{dm}\frac{d}{dt}i_{dm} = V_{dm} - R_m i_{dm} + p_m \omega_m L_{qm} i_{qm} \,, \tag{8a}$$

$$L_{qm}\frac{d}{dt}i_{qm} = V_{qm} - R_m i_{qm} - p_m \omega_m (L_{dm} i_{dm} + \lambda_m) \tag{8b}$$

Parameter	Symbol	PMS motor
Stator resistance	R_m	$40\,\text{m}\Omega$
Stator inductances	L_{dm}, L_{qm}	0.2 mH
Rotor magnetic flux	λ_m	0.125 Wb
Moment of inertia	J_m	$0.05\,\text{kgm}^2$
Number of pole pairs	p_m	6

Fig. 2. Efficiency of the reversible PMS machine (generator = positive torque, motor = negative torque).

where i_d, V_d and i_q, V_q are the direct and quadrature components of stator currents and voltages respectively, ω_m is the rotor angular speed, while the other parameters are described in Table I [13]. In view of (8), the stator winding loss has been taken into account by the resistance R_m, whereas all the additional losses including Eddy current losses, hysteresis losses and bearing losses are modelled via a dissipation torque of the rotor as follows:

$$J_m \frac{d}{dt}\omega_m = \frac{3}{2}p_m\lambda_m i_{qm} + T_{lm} + T_{dm}(\omega_m) \qquad (9)$$

where J_m is the rotor inertia, T_{lm} is the load torque, $\frac{3}{2}p_m\lambda_m i_{qm}$ corresponds to the electromagnetic torque and $T_{dm}(\omega_m)$ is the dissipation torque approximated by:

$$T_{dm} \triangleq -8 \times 10^{-5}\,\omega_m^2 + 2.2 \times 10^{-2}\,\omega_m - 2.86.$$

to provide a realistic representation of the machine efficiency as compared to data available in the literature [13].

Further simplification is also performed for ease of implementation: 1) transient currents are neglected because they have much faster dynamics than the mechanical dynamics; 2) $i_d = 0$ for the given control strategy; 3) the inertia torque $J\frac{d}{dt}\omega$ is neglected as it is reasonably smaller than the load torque in normal operating conditions. Hence, the dynamic model (8), (9) is suitably simplified into steady state, algebraic equations as follows:

$$V_{qm} - R_m i_{qm} - p_m\omega_m\lambda_m = 0, \qquad (10a)$$

$$\frac{3}{2}p_m\lambda_m i_{qm} + T_{lm} + T_{dm}(\omega_m) = 0. \qquad (10b)$$

which can be algebraically solved in terms of V_{qm} and i_{qm}, leading to the following expressions:

$$P_m = \omega_m T_{lm}, \qquad (11a)$$

$$P_i = \frac{3}{2}V_{qm}\,i_{qm} \qquad (11b)$$

$$= \omega_m(T_{lm} + T_{dm}) - \frac{2}{3}R_m\frac{(T_{lm} + T_{dm})^2}{(p_m\lambda_m)^2}. \qquad (11c)$$

Therefore the motor efficiency:

$$\eta_m = (P_m/P_i)^{\text{sign}(P_i)} \qquad (12)$$

can be explicitly evaluated as a function of the load torque T_{lm} and speed ω_m, as shown in Fig. 2. The PMS machine has an overall very high efficiency and the efficiency drops dramatically only at low speeds and torques.
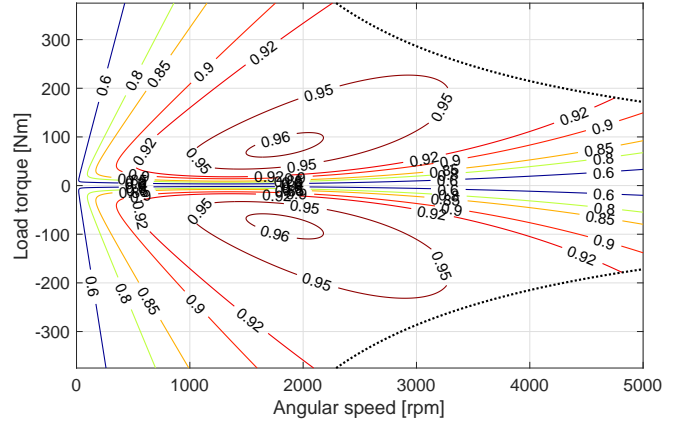
2) Transmission: In most cases, a series HEV is equipped by a fixed transmission (FT) because of the high operating efficiency of PMS motor in a wide range of speeds. It is well known that the FT is characterized by higher transmission efficiency and reduced mechanical complexity compared to a CVT. However, the appropriate selection of CVT transmission ratio makes it possible to operate the electric motor with higher efficiency. We will show that the CVT power losses are more than compensated by motor efficiency increase, leading in conclusion to a greater efficiency for the overall transmission even if the FT is more efficient than CVT efficiency. For the sake of further analysis, let us introduce the transmission equation, which has the same format for both mechanisms:

$$\omega_m/N = \omega_w = v/r_w \qquad (13)$$

where ω_w is the angular speed of the wheels, r_w is the wheel radius and v is the vehicle longitudinal speed. N is the gear ratio, that is fixed for FT whereas the CVT is enabled to achieve values of N in the range $2.13 - 12.7$ (that is taken from Nissan XTRONIC CVT [14]). In the following, we use suffix c and f respectively for CVT and fixed transmission (i.e., N_c and N_f). The bi-directional power flow is hence modeled with the following equation:

$$P_t = \eta_t^{\text{sign}(P_m)} P_m \qquad (14)$$

with η_t denotes the transmission efficiency. Without loss of generality, we assume the average efficiency of the CVT and FT are respectively 0.93 and 0.97 [15], [16].

3) Vehicle longitudinal dynamics: The gross motion of the vehicle is described in terms of speed u and yaw rate Ω, by using the single-track vehicle model. The longitudinal dynamics is described by the following differential equation:

$$m\frac{d}{dt}v = F_v - F_R - F_D \qquad (15)$$

where m is the overall mass, $F_R = 70\text{N}$ is the resistance force due to tires, $F_D = 0.47v^2$ is the aerodynamics drag resistance and $F_v = \frac{P_t + P_h}{v}$ represents the longitudinal driving force. P_h is mechanical brakes power that is always negative for deceleration.

The travelled distance s is obtained by integrating the longitudinal speed:

$$\frac{d}{dt} s = v . \tag{16}$$

While driving on public roads, it is reasonable to assume that the vehicle is driven in the middle of the lane for the entire drive mission. The road is thus defined in terms of curvature $\Theta(s)$ of the road center, which is calculated from its Cartesian coordinates as a function of the travelled distance s:

$$\Theta(s) = \sqrt{\left(\frac{d^2 x}{ds^2}\right)^2 + \left(\frac{d^2 y}{ds^2}\right)^2} . \tag{17}$$

Thus, the vehicle yaw rate Ω is simply computed by: $\Omega = v \, \Theta(s)$, and the vehicle turning can be modeled as $w \, \Omega = v \tan \delta$, where δ is the steering angle and w the wheelbase. From a practical perspective, the above assumption is not representative of drivers' behavior at sharp corners, which in the simulation are smoothed by properly filtering the curvature $\Theta(s)$.

D. Overall Powertrain model

Now, all the individual components are assembled to form the full powertrain model. From (6), (7), (12) and (14), the vehicle power flow is described with respect to three independent sources of power P_b, P_g, and P_h (corresponding respectively to the battery, generator, and brakes):

$$\begin{aligned}
P_r &= \eta_r P_g, \qquad P_{bl} = \eta_{dc}^{-\operatorname{sign} P_b} P_b \\
P_i &= \eta_i^{\operatorname{sign}(\eta_r P_g + P_b)} (\eta_r P_g + P_b) \\
P_t &= (\eta_i \eta_m \eta_t)^{\operatorname{sign}(\eta_r P_g + P_b)} (\eta_r P_g + P_b)
\end{aligned} \tag{18}$$

where $\eta_r, \eta_{dc}, \eta_i$ are constant, while η_m depend on the operating conditions (i.e., speed and torque of the motor). From a practical perspective, P_g, P_b, P_h are not controlled directly, but via the time derivatives j_g, j_b and j_h (which have the dimensions of jerk) of the power associated force F_g, F_b, F_h, to ensure smooth controls and to avoid unrealistic jerky manoeuvres. Moreover, the three independent power sources are calculated by $P_g = F_g v$, $P_b = F_b v$, $P_h = F_h v$. For the same reason, the CVT gear ratio N_c is also controlled by its time derivative j_n. The following system is obtained by collecting (1), (4), (15), (16) and the time derivatives of F_g, F_b, F_h and N_c:

$$\frac{d}{dt} \begin{pmatrix} Q_f \\ SoC \\ v \\ s \\ F_g \\ F_b \\ F_h \\ N_c \end{pmatrix} = \begin{pmatrix} q_{f0} + P_g/(Q_{HV} \, \alpha_f) \\ -i_b/Q_{max} \\ (P_t + P_h)/(m \, v) - (F_R + F_D)/m \\ v \\ m \, j_g \\ m \, j_b \\ m \, j_h \\ j_n \end{pmatrix} \tag{19}$$

III. OPTIMAL CONTROL PROBLEM FORMULATION

In this optimization framework, the drive mission is defined in terms of route with specified travelling time, determined by the assigned average speed. This is a very significant feature for real-time implementation because the drive cycle is not practically available. The objective of the optimal control strategy is to optimize fuel consumption by means of a proper power split, speed profile and CVT gear ratio (only first two for FT).

Let T denote the time instant when the vehicle completes the given trip, such that $T = L/v_{ave}$, with L the length of path and v_{ave} the requested average speed. The optimal control problem (OCP) is then formulated to find the power inputs as well as the proper CVT gear ratio $\mathbf{u} = [j_g, j_b, j_h, j_n]^T$ and speed profile that minimize fuel consumption $Q_f(T)$:

$$\min_{\mathbf{u}} Q_f(T) \tag{20a}$$

$$\text{subject to:} \quad \frac{d}{dt}\mathbf{x} = \mathbf{f}(\mathbf{x}, \mathbf{u}, t) \tag{20b}$$

$$\psi(\mathbf{x}, \mathbf{u}, t) \le \mathbf{0} \tag{20c}$$

$$\mathbf{b}(\mathbf{x}(0), \mathbf{x}(T)) = \mathbf{0} \tag{20d}$$

More specifically, the system model (20b) has already been specified in (19) with

$$\mathbf{x} = [Q_f, SoC, v, s, F_g, F_b, F_h, N_c]^T .$$

Inequality constraints (20c) are used to keep the operating conditions of the powertrain inside their admissible range, and to guarantee the driving safety and comfort. To this end, (20c) is the combination of all the following constraints. The limitation of the generator power is:

$$0 \le P_g \le P_{g,max} \tag{21}$$

The battery SoC are constrained:

$$SoC_{min} < SoC < SoC_{max} \tag{22}$$

and the current is constrained by the charging and discharging C-rate limits. The PMS motor (and indirectly the inverter) is constrained in terms of voltage and current:

$$V_{dm}^2 + V_{qm}^2 \le \frac{V_{dc}^2}{3}, \quad -i_{max} \le i_{qm} \le i_{max} \tag{23}$$

with $i_{max} = 200\text{A}$ and $V_{dc} = 700\text{V}$ Braking power is constrained to be negative:

$$P_h \le 0 \tag{24}$$

Driving speed constraint is:

$$v_{min} \le v \le v_{max} \tag{25}$$

where v_{max} is the legal speed limit. v_{min} is a small constant introduced to avoid the issue of singularity when the power is divided by v.

For driving safety, the longitudinal and lateral acceleration are constrained within an acceleration diamond [17] described as follows:

$$\left| \frac{F_v/m}{a_{x,max}} \right| + \left| \frac{v\Omega}{a_{y,max}} \right| \le 1 \tag{26}$$

with $a_{x,max}$ and $a_{y,max}$ are respectively the longitudinal and the lateral acceleration accepted by the driver. Finally, j_g, j_b, j_h are bounded within $\pm 1 \, m/s^3$, whereas j_n is also bounded within ± 1 for smooth control.

The initial and terminal conditions of the states are defined by the boundary conditions (20d). More specifically, the vehicle speed is assumed identical at the begin and at the end of the trip, such that $v(0) = v(T) = v_{min}$, and the trip is completed within the given time $s(T) - s(0) = L$. The charge sustaining condition is imposed on the operation of the battery, such that $SoC(0) = SoC(T)$. The boundary conditions of the force produced by the power sources are $F_g(0) = F_g(T) = F_b(0) = F_b(T) = F_h(0) = F_h(T) = 0$.

The OCP defined in (20) is addressed by a C++ based indirect solver [7], named PINS. This indirect method numerically solves the OCP via the associated boundary value problem (BVP) resulting from the PMP. It has already been shown that the indirect approach offers the same computational efficiency and accuracy as compared to the direct approaches (e.g., nonlinear programming), when provided with a finite difference approximation of the BVP and a robust nonlinear solver. More details on the adopted approach may be found in [7], [18].

IV. Numerical Examples

In this section, numerical examples are given to show the effectiveness of the CVT in a series hybrid vehicle by using fixed transmission as a benchmark. For the sake of comparison, a proper gear ratio has to be predefined for FT. With the aim of finding a single gear ratio for FT that is optimized for mixed driving situations, we consider a simple drive mission on a 1km straight path. The vehicle is requested to drive at an average speed of 50km/h, which is the same as that of the WLTP drive cycle [1]. The WLTP profile that consists of four speed dependent stages from low to extra high, is developed based on the real world driving data, therefore showing an improvement over conventional cycles, such as NEDC.
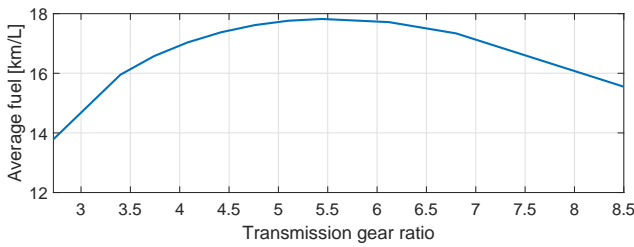
Fig. 3. Vehicle fuel economy with variable FT gear ratios for the 1km drive mission. The most fuel efficient gear ratio is 5.44.
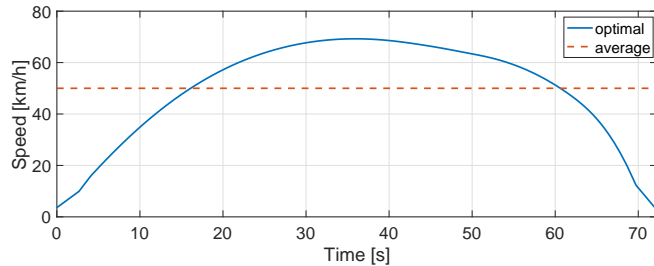
Fig. 4. Optimal speed profile obtained by the most fuel efficient gear ratio for FT.

The optimal control problem defined in the previous

[1] average speed of WLTP is 53.5km/h without stops and is 46.5km/h with stops

Section are solved by the simultaneous optimization of the driving speed and the power split. As can be seen in Fig. 3, the optimal gear ratio in terms of fuel economy is 5.44 for this proposed drive mission. Hence, N_f is fixed to be 5.44 for the upcoming comparisons. The driving speed profile for this most fuel efficient FT gear ratio is shown in Fig. 4. The optimal driving speed combines rapid acceleration at the beginning and a period of coasting after the vehicle reaches a maximum velocity. Such a speed pattern can be identified as pulse-and-glide, which has been proven to be most fuel efficient driving strategy for conventional vehicles.

Next, we consider a drive mission that requests the vehicle to travel at an average speed of 65km/h on a 6.8 km long rural route with scarce traffic (see Fig. 5). In this connection, the influence of other road users is neglected, and a constant legal limit 80km/h is imposed for simplicity. The road geometry defined in the geographic coordinate system has been converted into the curvature model, where the altitude is omitted for this flat road and the edges are smoothed by: $|\Theta| < 0.1 \, m^{-1}$.

Fig. 5. The route selected for the vehicle mission from A to B.

Next, the OCP solutions obtained in both scenarios are compared to show the benefit of the CVT in this series hybrid architecture. As shown in Fig. 6, the optimal driving speed is influenced by the transmission system, and the CVT embedded vehicle admits faster acceleration in general without losing energy efficiency. This is mainly because the CVT is capable to adapt the gear ratio to variable driving speeds. On the other hand, the optimal CVT drive ratio is regulated according to the speed in order to keep the motor to be operated efficiently. More specifically, a large gear ratio is employed when the velocity is low to avoid inefficient operation region of the motor, whereas the lower gear ratios correspond to the higher driving speed values.

Next, the operation of the motor throughout the trip is plotted in Fig. 7. It is observed that the CVT offers very steady motor efficiency around 0.92 by continuously optimizing the CVT gear ratio N_c. Conversely, the operating points are much more scattered when the FT is deployed, the motor is more efficient at some time instants, while majority of operating points are concentrated within 0.8–0.85. It is worth noting that the relationship between motor speed and torque in the presence of the CVT might be fitted by straight lines respectively for motoring and generating, leading to some heuristic control rules that are more computationally friendly. Such aspect is beyond the scope of the present work, and may be addressed in a further paper.

Fig. 8 shows the comparative results of the energy losses for the entire trip. As can be noticed, the CVT system improves the motor efficiency by reducing friction losses, and the associated optimal speed profile gives rise to reduced aerodynamic drag and tyre fiction losses. Eventually, the CVT successfully compensates the inferior transmission efficiency, and ends up with a higher overall efficiency than the FT. By utilizing the state Q_f, the average fuel is computed by $L/(Q_f(T)/\rho)$ with $\rho = 0.75$ the density of gasoline. The vehicle has the fuel economy of 17km/L in the presence of the FT, whereas the CVT improves the result by 3.53%, leading to 17.6km/L for the given drive mission. For the sake of completeness, further simulations are carried out showing that the CVT would persistently benefit the fuel economy until its efficiency falls below 0.9.
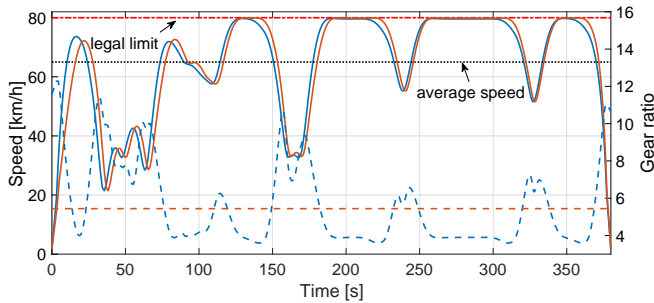

Fig. 6. Optimal driving speed and the associated gear ratio for vehicle systems using CVT (blue) and FT (red).
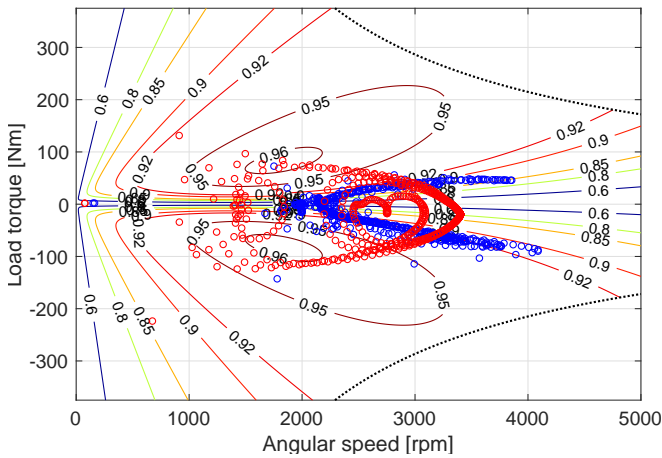

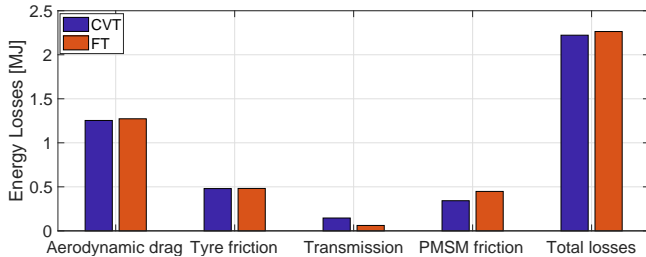Fig. 7. Operation of the motor for the CVT (blue) and FT (red) cases.

Fig. 8. Comparison of energy losses for vehicle systems using CVT (blue) and FT (red).

V. CONCLUDING REMARKS

In this paper, the performance of a CVT in a series hybrid architecture is investigated by comparing to the widely used FT. An optimal control methodology is adopted to address the optimization tasks of CVT, speed and power split. It has been shown by simulations that the CVT outperforms the FT in terms of overall efficiency for the selected urban drive mission, and improves the fuel economy by 3.53%. The results are mainly limited by the simplistic drive mission and CVT model. Future work consists in developing heuristic CVT control strategies for practical implementation by studying the optimal behavior of the motor and CVT in combination. Moreover, the driving mission can be extended by involving combined driving situations with variable speed limits. It is expected that the CVT can offer more improvement by fully exploiting the flexibility of variable gear ratio.

REFERENCES

[1] P. Bowles, H.Peng, and X. Zhang., "Energy management in a parallel hybrid electric vehicle with a continuously variable transmission," in *Proc. 2000 American Control Conference*, 2000, pp. 55–59.

[2] J.-S. Won, R. Langari, and M. Ehsani, "An energy management and charge sustaining strategy for a parallel hybrid vehicle with cvt," *IEEE Transactions On Control Systems Technology*, vol. 13, no. 2, pp. 313–320, 2005.

[3] H. Lee and H. Kim, "Improvement in fuel economy for a parallel hybrid electric vehicle by continuously variable transmission ratio control," *Proceedings of the Institution of Mechanical Engineers, Part D: Journal of Automobile Engineering*, vol. 219, no. 1, pp. 43–51, 2005.

[4] A. A. Mukhitdinov, S. K. Ruzimov, and S. L. Eshkabilov., "Optimal control strategies for cvt of the hev during a regenerative process," in *IEEE conference on Electric and Hybrid Vehicles*, 2006.

[5] N. Murgovski, L. M. Johannesson, and B. Egardt, "Optimal battery dimensioning and control of a cvt phev powertrain," *IEEE Transactions on Vehicular Technology*, vol. 63, no. 5, pp. 2151–2161, 2014.

[6] W. Shabbir and S. Evangelou., "Efficiency analysis of a continuously variable transmission with linear control for a series hybrid electric vehicle," in *19th World Congress of the IFAC*, 2014, pp. 6264–6269.

[7] F. Biral, E. Bertolazzi, and P. Bosetti, "Notes on numerical methods for solving optimal control problems," *IEEJ Journal of Industry Applications*, vol. 5, no. 2, pp. 154–166, 2016.

[8] R. Lot and S. A. Evangelou, "Green driving optimization of a series hybrid electric vehicle," in *52nd IEEE Conference on Decision and Control*, 2013, pp. 2200–2207.

[9] C. M. Shepherd, "Design of primary and secondary cells - part 2. an equation describing battery discharge," *Journal of Electrochemical Society*, vol. 112, pp. 657–664, July 1965.

[10] O. Tremblay and L. A. Dessaint, "Experimental validation of a battery dynamic model for ev applications," *World Electric Vehicle Journal*, vol. 3, 2009.

[11] M. Pahlevaninezhad, P. Das, J. Drobnik, P. K. Jain, and A. Bakhshai, "A novel zvzcs fullbridge dc/dc converter used for electric vehicles," *IEEE Trans. on Power Electronics*, pp. 2752–2769, 2012.

[12] P. Pillay and R. Krishnan, "Modelling, simulation, and analysis of permanent-magnet motor drives, Part I: The permanent-magnet synchronous motor drive," *IEEE Transactions on Industry Application*, vol. 25, no. 2, pp. 265–273, 1989.

[13] S. A. Evangelou and A. Shukla, "Advances in the modelling and control of series hybrid electric vehicles," in *American Control Conference, 2012. Proceedings of the*, 2012.

[14] "Nissan xtronic cvt," *[Online]. Available: http://www.nissan-global.com/EN/DOCUMENT/PDF/ENVIRONMENT/TECHNOLOGY/en_xtronic_ura.pdf*.

[15] J. M. Miller, *Propulsion Systems for Hybrid Vehicles*. The Institution of Engineering and Technology, 2003.

[16] R. Heath, "Seamless amt offers efficient alternative to cvt," in *JSAE Annu. Congr.*, 2007.

[17] F. Biral, M. Da Lio, and E. Bertolazzi, "Combining safety margins and user preferences into a driving criterion for optimal control-based computation of reference maneuvers for an adas of the next generation," *IEEE Intelligent Vehicles Symposium, Proceedings*, vol. 2005, pp. 36–41, 2005.

[18] E. Bertolazzi, F. Biral, and M. Da Lio, "Symbolic-numeric efficient solution of optimal control problems for multibody systems," *Journal of Computational and Applied Mathematics*, vol. 185, no. 2, pp. 404–421, 2006.